Time-Resolved Fluorescence Anisotropy Study of Effect of a Cis Double Bond on Structure of Lecithin and Cholesterol–Lecithin Bilayers Using *n*-(9-Anthroyloxy) Fatty Acids as Probes†

Michel Vincent* and Jacques Gallay

ABSTRACT: The *n*-(9-anthroyloxy) fatty acid fluorescent probes have been previously studied by the time-resolved anisotropy technique in dipalmitoylphosphatidylcholine vesicles with regard to isotropic solvents [Vincent, M., de Foresta, B., Gallay, J., & Alfsen, A. (1982) *Biochemistry 21*, 708–716]. In the present work, we have investigated the effect of a single cis double bond on the dynamics and order of lipid bilayer in vesicles of 1-palmitoyl-2-oleyl-*sn*-glycero-3-phosphocholine with this set of probes, which report the microenvironment at a graded series of depths from the surface to the center of the bilayer. The ordering of the hydrocarbon chains and the local "microviscosity" can be evaluated respectively from the nonzero constant value (r_∞) of the anisotropy decay curve and from the correlation time ρ_{0p} computed from the steady-state anisotropy at 319 nm as excitation wavelength, at which the anisotropy decay is asymptotic to zero. In the gel phase (−10 °C), these probes evidence the existence of three regions through the bilayer. The ordering of the hydrocarbon chains increases from 2- to 7-AS, decreases from 7- to 12-AS (double-bond region), and increases from 12-AS to 16-AP. The "microviscosity" is the highest in the seventh carbon region. In the liquid-crystalline phase (10 °C), the microviscosity is also the highest in the seventh carbon region. Upon addition of cholesterol, no ordering effect occurs in the gel phase in the second carbon region, i.e., near the aqueous interface. An enhancement of the ordering is evidenced in the seventh to ninth carbon region. The disordering of the hydrocarbon chains in the 12th carbon region observed in absence of cholesterol disappears. In the 16th carbon region, cholesterol has a strong disordering effect on the hydrocarbon chains. Upon addition of cholesterol, the microviscosity in the gel phase as well in the liquid-crystalline phase is enhanced with a maximum in the seventh to ninth carbon region.

A detailed knowledge of the structure and dynamics of the lipid molecules in biological membranes is essential for the understanding of membrane functions and cellular activities. For this purpose, the phospholipid bilayer has been extensively used as a model membrane system. In particular, the structural and dynamical changes that accompany the gel → liquid crystalline phase transition have been studied by employing a wide variety of physical techniques.

The effect of acyl chain unsaturation in model systems has been previously examined by deuterium NMR[1] (Seelig, 1977) and ESR (Griffith & Jost, 1976). An increase of the rate of motion and a decrease of the order parameter of the acyl chains were observed upon introduction of a single cis double bond in the lecithin molecules. In monolayer studies, the extent and number of double bonds were shown to be of importance for the interaction of phospholipid with cholesterol (Demel et al., 1972; Ghosh & Tinocco, 1972; Evans & Tinocco, 1978).

Fluorescence technique has been also employed to study the influence of unsaturation on the dynamic properties of the acyl chain (Lentz et al., 1976; Stubbs et al., 1981). In the case of DPH, the uncertainty about the location of this probe is one of the difficulties of interpretation (Zannoni et al., 1983; Lakowicz & Knutson, 1980). Due to their structural analogy with the membrane lipid components, the *n*-(9-anthroyloxy) fatty acids are likely to fit in the membrane with their acyl chain parallel to those of the phospholipids. These probes allow a labeling at a graded series of depth in the bilayer, as demonstrated by fluorescence quenching and energy-transfer experiments (Thulborn & Sawyer, 1978; Haigh et al., 1979). With this set of fluorescent probes, a "microviscosity barrier in the lipid bilayer due to the presence of phospholipid containing unsaturated acyl chains" has been evidenced (Thulborn & Sawyer, 1978). However, only the steady-state mode was employed by these authors.

In this work, the effect of unsaturation was examined on POPC vesicles with the *n*-(9-anthroyloxy) fatty acid probes, by time-resolved fluorescence anisotropy. This was performed at two excitation wavelengths, which is prerequisite for separating the two depolarizing motions of the fluorophore, i.e., the in-plane and out-of-plane modes of rotation. These investigations were focused on the estimation of the degree of packing of the phospholipid acyl chains at different depths within the bilayer as modified by unsaturation. This was performed at different temperatures above and below the transition temperature of POPC vesicles and in mixed cholesterol–POPC vesicles (0.20 and 0.33 mol fraction).

Materials and Methods

Chemicals. 1-Palmitoyl-2-oleyl-*sn*-glycero-3-phosphocholine (POPC) (Sigma, St. Louis, MO) and 1,2-dipalmitoyl-*sn*-glycero-3-phosphocholine (DPPC) (Serdary, Canada) were used as purchased. Each of these chemicals migrated as a single spot on silica with chloroform–methanol–water (65:25:5 v/v/v) as solvent. Glycerol was from Merck (Darmstadt,

† From Equipe de Recherche No. 64 du Centre National de la Recherche Scientifique and Unité 221 de l'Institut National de la Santé et de la Recherche Médicale, Unité d'Enseignement et de Recherche Biomédicale des Saints-Pères, Université Paris V, 75270 Paris Cedex 06, France. *Received December 6, 1983; revised manuscript received May 10, 1984.* This work was supported in part by Grant CRL 813035 from INSERM. This work is part of the Doctorat d'Etat of M.V.

* Address correspondence to the author at ER64 CNRS, 45 rue des Saintes-Pères, 75270 Paris Cedex 06, France.

[1] Abbreviations: DPPC, 1,2-dipalmitoyl-*sn*-glycero-3-phosphocholine; DOPC, 1-palmitoyl-2-oleoyl-*sn*-glycero-3-phosphocholine; *n*-AS, *n*-(9-anthroyloxy)stearic acid (*n* = 2, 7, 9, and 12); 16-AP, 16-(9-anthroyloxy)palmitic acid; NMR, nuclear magnetic resonance; ESR, electron spin resonance; DPH, 1,6-diphenyl-1,3,5-hexatriene; MWR, mean weighted residue.

0006-2960/84/0423-6514$01.50/0

Germany) and was free of fluorescent impurities. Cholesterol (Serva, Germany) was used as supplied. *n*-(9-Anthroyloxy) fatty acids were from Molecular Probes (Plano, CA). Their purity was controlled by thin-layer chromatography with ethanol–water (95:5 v/v) as solvent. DPH was from Koch Light Laboratories (Colnbrook Bucks, England). All other reagents were of the highest grade commercially available.

Phospholipid and Cholesterol–Phospholipid Samples. Ethanol-injected vesicles were prepared by the method of Kremer et al. (1977) from 30 mg/mL ethanolic solutions of POPC, with or without cholesterol (0.20 and 0.33 mol fraction). The injection of 600 μL of these ethanolic solutions in 20 mL of 0.01 M Tris-HCl buffer, pH 8, 0.1 M NaCl, and 25% (v/v) glycerol was performed above the transition temperature. Buffer was degassed and saturated with argon before use. The sample was passed through a 450-nm Millipore filter. Lipid vesicles were labeled by adding 3 μL of a 1 mg/mL tetrahydrofuran solution of *n*-(9-anthroyloxy) fatty acids in 3 mL of buffer containing the vesicles (probe to phospholipid molar ratio $\simeq 1/400$). One blank was performed by adding the same tetrahydrofuran aliquot without fluorescent probe to the lipid vesicle suspension. DPPC vesicles were prepared as previously described (Vincent et al., 1982a). In the experiments with DPH as fluorescent probe, the probe to phospholipid molar ratio was $\simeq 1/500$.

Steady-State Fluorescence Measurements. The steady-state fluorescence emission anisotropies were measured with a T-format SLM 8000 spectrofluorometer (Urbana, IL) equipped with a single-grating excitation monochromator (MC 320) and Glan-Thompson polarizers. The sample cell holder was regulated by a Hüber HS 40 thermostat. Temperature in the sample was checked by means of a Digitec 5810 digital thermometer (Dayton, OH). The band-pass was set to 2 nm, and fluorescence emission was collected through Schott KV 418 cutoff filters for DPH as well as for the *n*-(9-anthroyloxy) fatty acids. The emission anisotropies were calculated according to

$$r = [R(\text{vert}) - R(\text{horz})]/[R(\text{vert}) + 2R(\text{horz})]$$

where $R(\text{vert}) = I_{vv}/I_{vh}$ and $R(\text{horz}) = I_{hv}/I_{hh}$, the first and the second subscripts referring to excitation and emission components, respectively. These relative intensities were directly recorded with the ratio mode in order to eliminate source intensity fluctuations. $R(\text{horz})$ is a calibration factor, which normalizes the output response of each analysis channel. When necessary, the contribution of scattering to the fluorescence intensity can be automatically subtracted on each channel, leading to the corrected new ratios:

$$R(\text{vert}) = (I_{vv} - I'_{vv})/(I_{vh} - I'_{vh})$$

and

$$R(\text{horz}) = (I_{hv} - I'_{hv})/(I_{hh} - I'_{hh})$$

where the prime refers to the blank. Calculation of rotational correlation time at 319 nm was performed from $\rho = \tau/(r_0/r - 1)$ (Weber, 1971) with $r_0 = 0.1$. The error on this parameter was determined from $\Delta r = \Delta r_0 = \pm 0.001$ and by neglecting error on $\langle\tau\rangle$.

Nanosecond Anisotropy Decay Measurements. The time courses of the emission anisotropy were obtained with a single photon counting fluorometer (Applied Photophysics System SP7 and Ortec 9200 electronic device), as previously described (Gallay et al., 1981, 1982). Excitation wavelength was selected by a grating monochromator. Emission was collected through a Schott KV 418 cutoff filter. Glan-Thompson polarizers were used on excitation and emission sides. The flash lamp was filled with air under a pressure of 0.5 atm. The spectral lines obtained at 316 (the closest to 319 nm, where $r_0 = 0.1$) and 381 nm were used for the excitation of *n*-(9-anthroyloxy) fatty acids, and the one at 337 nm was used for the excitation of DPH. The emission decay curves $I_{vv}(t)$ and $I_{vh}(t)$ of the sample, from which a blank was subtracted when needed, were collected successively. The experimental sum, $s(t)$, and difference, $d(t)$, decays were calculated from the data according to

$$s(t) = I_{vv}(t)G + 2I_{vh}(t)$$
$$d(t) = I_{vv}(t)G - I_{vh}(t)$$

where G is a correction factor for the fluctuations in excitation intensity and for the difference in the response of the analysis photomultiplier to differently polarized light; G is given by

$$G = [(1 + 2r)/(1 - r)][\textstyle\sum I_{vh}(t)/\sum I_{vv}(t)]$$

where r is the steady-state anisotropy of the sample determined as described above and $\sum$ refers to the summation of the counts for each curve over all the analyzer channels (Dale et al., 1977).

The impulse responses $S(t)$ and $D(t)$ are related to the experimental functions $s(t)$ and $d(t)$ by the convolution integrals:

$$s(t) = \int_0^t S(t - t')g(t')\,dt'$$

and

$$d(t) = \int_0^t D(t - t')g(t')\,dt'$$

where $g(t')$ is the apparatus response function. A mono- or biexponential decay is assumed for $S(t)$ and $D(t)$; their parameters are computed by using the modulation function method according to Valeur (1978), followed for $S(t)$ by a nonlinear least-squares regression analysis. A first approximation of the parameters of the anisotropy profile $r(t)$

$$r(t) = [I_{vv}(t) - I_{vh}(t)]/[I_{vv}(t) + 2I_{vh}(t)]$$

also assumed to be mono- or biexponential, is given by calculating the ratio $D(t)/S'(t)$, where $S'(t)$ is equal to $S(t)$ when this last function is monoexponential. When it is not the case, $S'(t)$ is chosen as $S'(t) = a' \exp(-t/\langle\tau\rangle)$, where $\langle\tau\rangle$ is the mean excited state lifetime calculated as $\langle\tau\rangle = \sum a_i\tau_i^2/\sum a_i\tau_i$ and $a' = \sum a_i$ (Chen et al., 1977). Starting from these calculated parameters of $r(t)$, a nonlinear least-squares regression is performed, fitting the convolution product of $g(t)$ by $r(t)$ to the experimental curve $d(t)$, in which the parameters of $S(t)$ are held constant and only those of the decay time components of $r(t)$ are adjusted. When one of the decay time components of $r(t)$ is long as compared to the mean excited state lifetime, a nonexponential function of the form

$$r(t) = r_1 \exp(-1/\phi) + r_\infty$$

can be used as a trial function for the analysis. r_1 can be written as

$$r_1 = r_{t=0} - r_\infty$$

where $r_{t=0}$ is the anisotropy at zero time. Data related to ϕ and r_∞ for DPH have been interpreted according to the "wobbling-in-cone" model (Kinosita et al., 1977) and to the distribution function theory (Lipari & Szabo, 1980; Heyn, 1979; Jähnig, 1979).

Results

Fluorescence Properties of n-(9-Anthroyloxy) Fatty Acid Probes in POPC Vesicles. Thermal scans of the steady-state

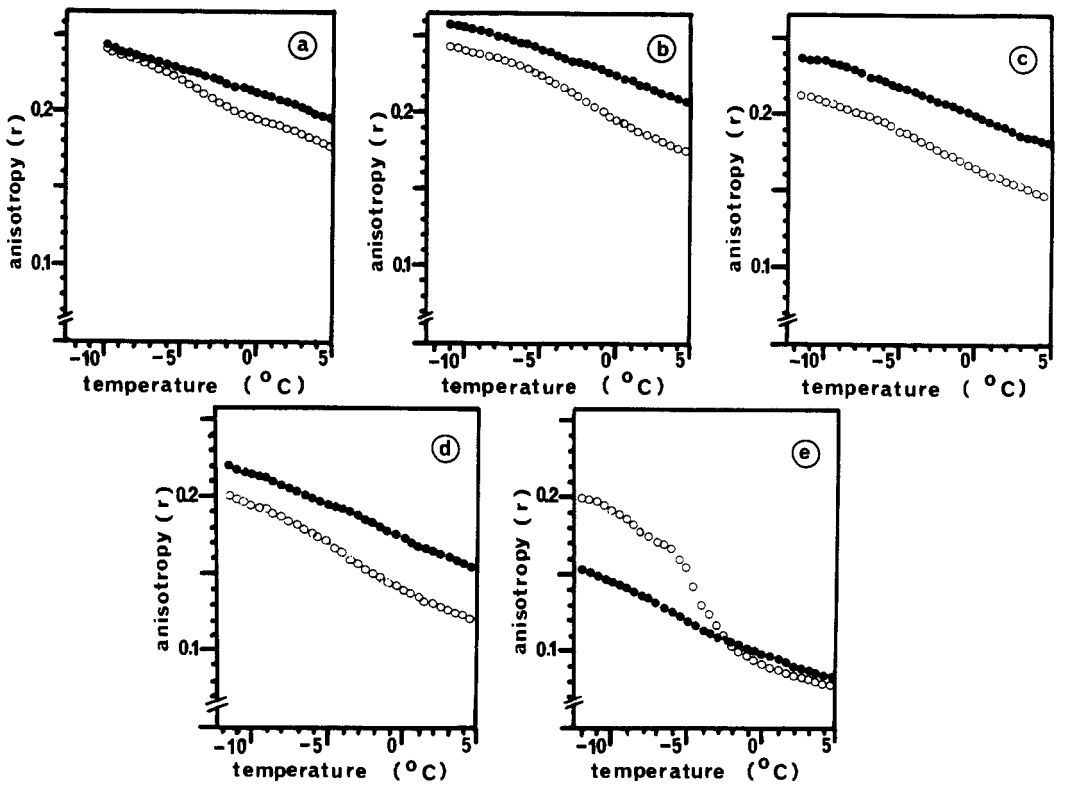

FIGURE 1: Plots of fluorescence emission anisotropy values vs. temperature for the phase transition of POPC vesicles without (○) or with cholesterol (●) (0.2 mol fraction): (a) 2-AS; (b) 7-AS; (c) 9-AS; (d) 12-AS; (e) 16-AP. Heating curves are presented. Excitation wavelength was set at 381 nm.

Table I: Parameters of Total Intensity Decays of *n*-(9-Anthroyloxy) Fatty Acids in POPC and POPC–Cholesterol Bilayers[a]

	probe	τ_1 (ns)[b]	A_1 (%)[b]	τ_2 (ns)[b]	A_2 (%)[b]	$\langle\tau\rangle$ (ns)[c]
POPC at −10 °C	2-AS	13.4 (0.9)[d]	0.52 (0.07)	5.1 (1.1)	0.48 (0.07)	11.3 (0.2)
	7-AS	14.7 (0.6)	0.61 (0.06)	6.0 (0.5)	0.39 (0.06)	12.8 (0.1)
	9-AS	15.8 (0.7)	0.58 (0.07)	7.3 (0.8)	0.42 (0.07)	13.7 (0.1)
	12-AS	16.9 (0.9)	0.58 (0.08)	7.2 (0.8)	0.42 (0.08)	14.6 (0.2)
	16-AP	19.2 (0.5)	0.53 (0.04)	10.1 (0.2)	0.47 (0.04)	16.3 (0.1)
POPC at 10 °C	2-AS	10.5 (0.5)	0.71 (0.03)	3.1 (0.6)	0.29 (0.03)	9.7 (0.3)
	7-AS	11.1 (0.3)	0.81 (0.09)	3.5 (0.7)	0.19 (0.09)	10.3 (0.4)
	9-AS	12.4 (0.3)	0.77 (0.03)	4.4 (0.9)	0.23 (0.03)	11.6 (0.3)
	12-AS	13.7 (0.4)	0.79 (0.06)	3.8 (0.8)	0.21 (0.06)	13.0 (0.4)
	16-AP	15.0 (0.5)	0.68 (0.08)	5.8 (0.7)	0.32 (0.08)	13.6 (0.2)
POPC–cholesterol at −10 °C	2-AS	12.2 (0.1)	0.59 (0.04)	2.9 (0.4)	0.41 (0.04)	10.9 (0.1)
	7-AS	13.2 (0.5)	0.62 (0.04)	4.4 (0.5)	0.38 (0.04)	11.6 (0.2)
	9-AS	15.4 (0.4)	0.37 (0.03)	6.6 (0.5)	0.63 (0.03)	11.7 (0.1)
	12-AS	16.4 (0.6)	0.35 (0.03)	8.4 (0.3)	0.65 (0.03)	12.5 (0.1)
	16-AP	22.3 (0.5)	0.16 (0.02)	12.3 (0.2)	0.84 (0.02)	14.8 (0.3)
POPC–cholesterol at 10 °C	2-AS	10.4 (0.3)	0.69 (0.04)	6.3 (0.5)	0.31 (0.04)	9.5 (0.2)
	7-AS	10.8 (0.4)	0.79 (0.06)	8.1 (0.5)	0.21 (0.06)	10.4 (0.3)
	9-AS	12.8 (0.1)	0.58 (0.04)	8.7 (0.4)	0.42 (0.04)	11.4 (0.3)
	12-AS	19.6 (0.5)	0.21 (0.03)	11.0 (0.2)	0.79 (0.03)	13.8 (0.2)
	16-AP	21.7 (0.4)	0.15 (0.04)	12.1 (0.4)	0.85 (0.04)	14.4 (0.3)

[a] Cholesterol/phospholipid = 0.33. [b] The total fluorescence intensity defined as $A_1 \exp(-t/\tau_1) + A_2 \exp(-t/\tau_2)$. [c] $\langle\tau\rangle$, the mean excited state lifetime, has been defined under Materials and Methods. [d] The values in parentheses denote standard deviation for at least three measurements.

fluorescence anisotropy of this set of probes embedded in POPC vesicles are presented in Figure 1. The excitation wavelength was selected at 381 nm. The thermal transition of the phospholipid occurs near −3 to −4 °C. This transition affects the steady-state anisotropy of the deepest probes (12-AS and 16-AP) more markedly than the other ones: 2-, 7-, and 9-AS. This was also observed for saturated lecithins (Thulborn & Sawyer, 1978). As previously observed in saturated lecithin vesicles (Vincent et al., 1982a), the total fluorescence intensity decays of the *n*-(9-anthroyloxy) fatty acid derivatives in POPC vesicles are fitted by a biexponential model in both the gel (−10 °C) and the liquid-crystalline phase (10 °C) (Table I, upper part). The values of both lifetimes appear to increase as a function of the substitution position along the acyl chain

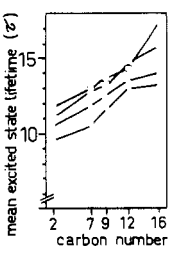

FIGURE 2: Mean excited state lifetime values at −14 (○), −5 (□), 5 (△), and 10 °C (▽) for the *n*-(9-anthroyloxy) fatty acid derivatives in pure POPC vesicles. Excitation wavelength was set at 381 nm.

whereas their respective weighing remains approximately constant ($A_1 = 0.56 \pm 0.04$, for the longer component). Both

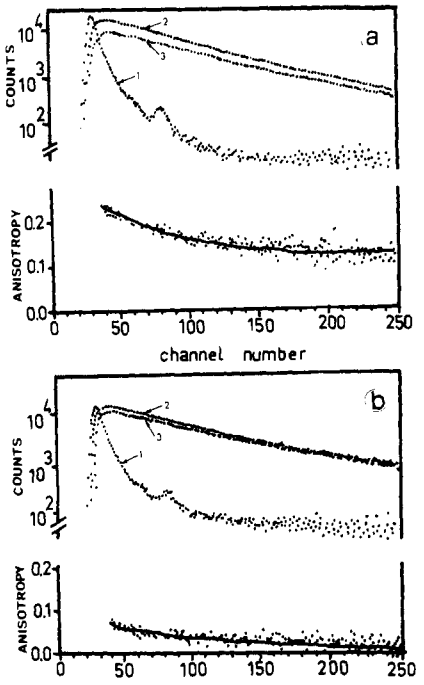

FIGURE 3: (a) (Upper part) Semilogarithmic representation of the experimental polarized decay curves $I_{vv}(t)$ (2) and $I_{vh}(t)$ (3) with the excitation pulse (1) for 9-AS in POPC vesicles at −10 °C. Time calibration was 0.249 ns per channel. Excitation wavelength was 381 nm. (Lower part) The experimental (···) and theoretical (—) curves for the decay of emission anisotropy. (b) As in (a) except the excitation wavelength was set at 316 nm.

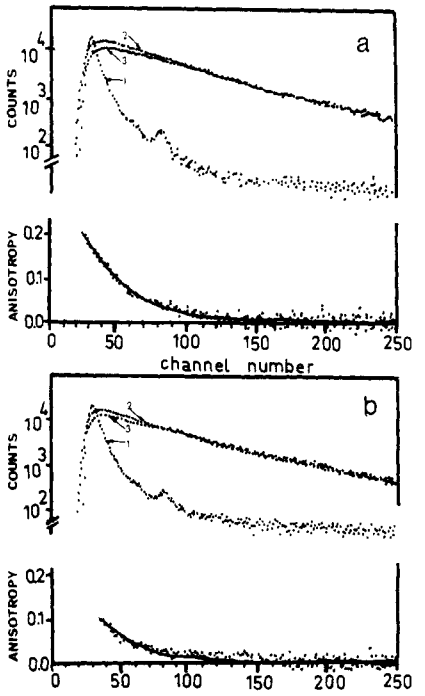

FIGURE 4: (a) (Upper part) Semilogarithmic representation of the experimental polarized decay curves $I_{vv}(t)$ (2) and $I_{vh}(t)$ (3) with the excitation pulse (1) for 9-AS in POPC vesicles at 10 °C. Time calibration was 0.249 ns per channel. Excitation wavelength was 381 nm. (Lower part) The experimental (···) and theoretical (—) curves for the decay of emission anisotropy. (b) As in (a) except the excitation wavelength was set at 316 nm.

time components exhibit shorter values in the liquid-crystalline phase. The variations of the mean excited state lifetime $\langle\tau\rangle$ behave accordingly (Figure 2). For each temperature, an increase of $\langle\tau\rangle$ is observed as a function of the bilayer penetration. A plateau value is obtained between the 12-AS and 16-AP probes at 5 and 10 °C while an enhancement of $\langle\tau\rangle$ between the 12-AS and 16-AP probes is observed at −5 °C and is more pronounced at −14 °C.

When the probes are excited at 316 nm at which the out-of-plane mode of rotation is monitored, the fluorescence anisotropy decays are asymptotic to zero, in both the gel phase (−10 °C) and the liquid crystalline phase (10 °C) (Figures 3 and 4). The computed values of the rotational correlation time $\rho_{op} = \langle\tau\rangle/(r_0/r - 1)$ at −10 and 10 °C are plotted in Figure 5. At both temperatures, a higher ρ_{op} value is observed for 7-AS. This effect is more pronounced at −10 °C.

When the excitation wavelength is selected at 381 nm, a nonzero asymptotic value of the anisotropy profile is observed below the transition temperature (Figure 3) and a few degrees above (0 and 5 °C) for each probe. The decays are fitted by a single exponential term plus a constant: $r(t) = (r_{t=0} - r_\infty)\exp(-t/\phi) + r_\infty$. The variation of the r_∞ value as a function of the temperature for the set of five probes is shown in Figure 6 (left part). At −14 and −10 °C, an increase of r_∞ is observed from 2-AS to 7-AS, followed by a decrease from 7-AS to 12-AS and again an increase from 12-AS to 16-AP. A few degrees below the transition temperature (−5 °C) and above (0 and 5 °C), the r_∞ values are constant as a function of the substitution position from 2-AS to 7-AS and decrease from 7-AS to 16-AP (Figure 6, left part). As a point of comparison, the values of r_∞ were measured at low temperature (−10 °C) in DPPC. A constant value from 2-AS to 16-AP is evidenced on Figure 6 (left part). The r_∞ values are higher in DPPC than in POPC at the same temperature.

The same figure (Figure 6, right part) shows the variations of the apparent rotational correlation time as a function of the

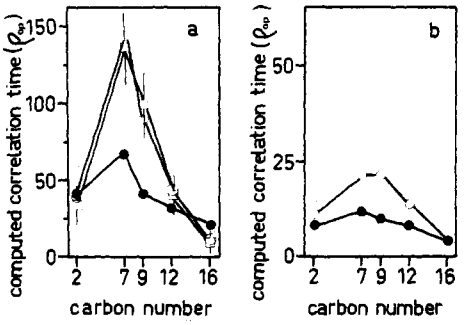

FIGURE 5: Computed correlation time values for *n*-(9-anthroyloxy) fatty acid derivatives in POPC vesicles (●), in cholesterol–POPC vesicles (0.2 mol fraction) (○), and in cholesterol–POPC vesicles (0.33 mol fraction) (□) at −10 (a) and 10 °C (b). The excitation wavelength was set at 319 nm, and details of computation and error bar calculation are described under Materials and Methods.

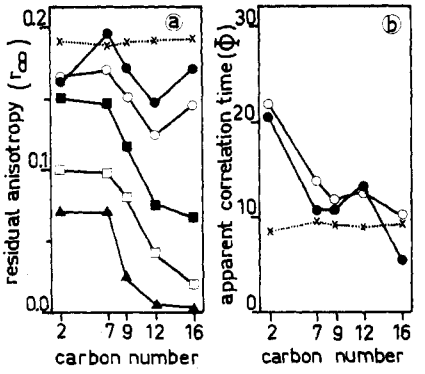

FIGURE 6: Parameters of anisotropy decays of *n*-(9-anthroyloxy) fatty acids monitored with 381-nm excitation wavelength. r_∞ and ϕ are from $r(t) = (r_{t=0} - r_\infty)\exp(-t/\phi) + r_\infty$. (a) Residual anisotropy values as a function of the temperature; (b) apparent correlation time values. The temperatures for both (a) and (b) are −14 (●), −10 (○), −5 (■), 0 (□), and 5 °C (▲). The same values r_∞ and ϕ for DPPC vesicles at −10 °C (×) are also presented.

Table II: Zero-Time Anisotropy Values Computed from Anisotropy Decays for *n*-(9-Anthroyloxy) Fatty Acids in POPC or POPC–Cholesterol Vesicles

	POPC at a temp (°C) of						POPC–cholesterol (0.2) at a temp (°C) of		POPC–cholesterol (0.33) at a temp (°C) of	
	−14	−10	−5	0	5	10	−10	10	−10	10
2-AS	0.29	0.27	0.27	0.27	0.26	0.24	0.26	0.24	0.27	0.24
7-AS	0.30	0.29	0.28	0.29	0.27	0.25	0.29	0.25	0.29	0.26
9-AS	0.29	0.29	0.28	0.28	0.25	0.23	0.29	0.23	0.30	0.25
12-AS	0.28	0.28	0.27	0.27	0.24	0.26	0.28	0.22	0.29	0.24
16-AP	0.31	0.27	0.25	0.21	0.20	0.22	0.23	0.17	0.25	0.18

substitution position and temperature. Below the transition (−14 and −10 °C), the general feature of the ϕ plot as a function of the location of the fluorophore is that it follows an opposite trend as compared to the r_∞ plot: a decrease from 2-AS to 7-AS, an increase from 7-AS to 12-AS, and a further decrease for 16-AP. For comparison, the values of ϕ in DPPC vesicles at −10 °C are shown on the same figure (Figure 6, right part); ϕ values are lower in DPPC than in POPC. Above the melting transition (10 °C), different models were tried to fit the $r(t)$ curves: (i) one exponential, (ii) two exponentials, and (iii) one exponential + a constant term. The values of the mean weighted residue (MWR) for all these models are anomalously high (about 10 as compared to typical range of 2–4 below the transition). This indicates that none of these models agrees with the experimental data. Nevertheless, the MWR value is the lowest for the double-exponential model. As already pointed out (Vincent et al., 1982a), the variations of $r_{t=0}$ (Table II) and r_∞ (Figure 6) follow a similar trend in agreement with other observations (Thulborn & Beddard, 1982).

Fluorescence Properties of n-(9-Anthroyloxy) Fatty Acids in Mixed POPC–Cholesterol Vesicles. The thermal dependence of the steady-state anisotropy of 2-, 7-, 9-, and 12-AS and 16-AP in POPC–cholesterol vesicles is shown in Figure 1. For the 7- to 12-AS probes, r is enhanced as compared to the pure POPC vesicles whatever the temperature (Figure 1). For the 2-AS, the effect of cholesterol is not significant in the gel phase. For the 16-AP probe the effect is dual: the cholesterol lowers the r values below the transition while a slight increase is observed above the transition temperature.

As in cholesterol-free POPC vesicles, the total fluorescence intensity decays are always best fitted with a biexponential model, whatever the probe. In these vesicles, the long time component exhibits comparable values as in the cholesterol-free vesicles except for the 16-AP in the gel phase and the 12-AS and 16-AP in the liquid-crystalline phase (Table I, lower part). There is an increase of the values of the shorter lifetime components, especially at 10 °C in the cholesterol POPC vesicles. The respective weighing of each time component appears to be dependent on the labeled depth at least in the deepest part of the membrane (Table I, lower part) where the weighing of the long time component falls to 15% for 16-AP at both temperatures (−10 and 10 °C). In Figure 7 are reported the variations of $\langle\tau\rangle$, the mean excited state lifetime. In the gel phase of the pure lipid (−10 °C), one can observe a slight decrease of $\langle\tau\rangle$, which is more pronounced in the deepest region of labeling (Figure 7). A reverse situation is found above the transition temperature of the pure lipid. The increase of the $\langle\tau\rangle$ values is more important in the deepest part of the bilayer (Figure 7).

The fluorescence anisotropy decays of the *n*-(9-anthroyloxy) probes with 316 nm as excitation wavelength (out-of-plane mode of rotation) are asymptotic to zero, whatever the probe and the temperature (data not shown), as in the case of pure

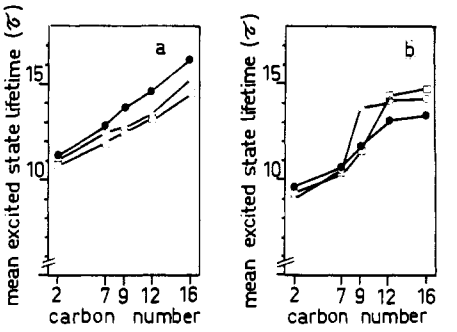

FIGURE 7: Mean excited state lifetime values at −10 (a) and 10 °C (b) for *n*-(9-anthroyloxy) fatty acid derivatives in POPC vesicles (●), cholesterol–POPC vesicles (0.2 mol fraction) (○), and cholesterol–POPC vesicles (0.33 mol fraction (□). The excitation wavelength was set at 381 nm.

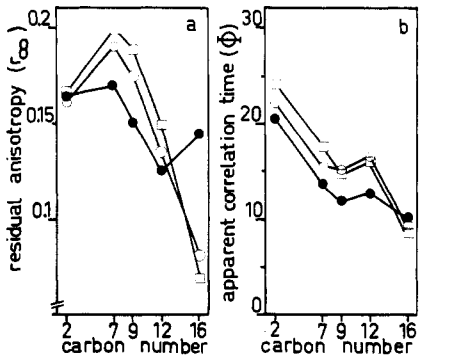

FIGURE 8: Residual anisotropy values (r_∞) (a) and apparent correlation time values (ϕ) (b) of anisotropy decays of *n*-(9-anthroyloxy) fatty acid probes. The excitation wavelength was set at 381 nm, and the temperature was −10 °C. (●) POPC vesicles; (○) cholesterol–POPC vesicles (0.2 mol fraction); (□) cholesterol–POPC vesicles (0.33 mol fraction).

POPC vesicles. The rotational correlation time values (ρ_{op}) as a function of the labeled level, cholesterol mole fraction, and temperature were computed. The results are shown in Figure 5. At −10 °C (left part), the presence of cholesterol enhances by about 2 times the ρ_{op} values of 7- and 9-AS observed in pure POPC vesicles. In contrast, for 2-AS, 12-AS, and 16-AP, no significant effect of cholesterol is evidenced (Figure 5). At 10 °C, cholesterol enhances ρ_{op} values except for 2-AS and 16-AP (Figure 5, right). The ρ_{op} values are lowered by about 6 times upon increasing the temperature from −10 to 10 °C.

With the excitation wavelength set at 381 nm, the fluorescence anisotropy decays of these probes reach a nonzero plateau value below the transition temperature of the pure lipid. The anisotropy profiles are fitted with an exponential term plus a constant term (r_∞). In Figure 8 are reported the r_∞ values for the five probes as a function of the cholesterol mole fraction. The variation of the r_∞ values as a function of carbon attachment presents a maximum at C_7. As com-

Table III: Decay Parameters for Total Emission[a] and for Anisotropy Emission[b] of DPH in Pure Vesicles and in Cholesterol-Containing POPC Vesicles[c]

	$\langle\tau\rangle_{(ns)}$	$r_{t=0}$	$\phi_{(ns)}$	r_∞	r	S	θ_{max} (deg)
POPC at −10 °C	10.0	0.37	9.7	0.316	0.342	0.91	20
POPC at 10 °C	8.8	0.32	7.1	0.057	0.172	0.38	60
POPC–cholesterol at −10 °C	10.0	0.37	9.2	0.301	0.335	0.89	22
POPC–cholesterol at 10 °C	9.7	0.33	5.4	0.178	0.233	0.68	40

[a] $\langle\tau\rangle$, the mean excited state lifetime, has been defined under Materials and Methods. [b] The fluorescence emission anisotropy $r(t) = r_{t=0}\exp(-t/\phi) + r_\infty$. The order parameter $S = (r_\infty/r_0)^{1/2}$; $r_0 = 0.384$ (Gallay et al., 1982). The wobbling in cone semiangle θ_{max} = arc cos $((1/2)[-1 + (8S + 1)^{1/2}])$. [c] Cholesterol/lipid = 0.2.

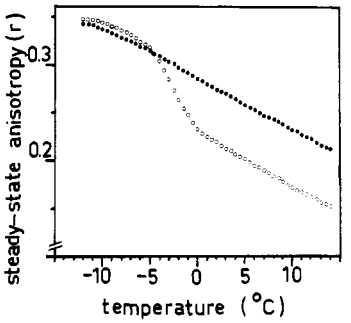

FIGURE 9: Plot of fluorescence emission anisotropy of DPH vs. temperature for phase transition of POPC vesicles without (○) or with cholesterol (●) (0.2 mol fraction). Heating curves are presented.

pared to pure POPC, no effect of the sterol is observed for the 2-AS probe (Figure 8, left part). The r_∞ values are increased for 7-, 9-, and 12-AS as a function of cholesterol content. In contrast, for the 16-AP probe, a large decrease of this parameter is observed upon addition of cholesterol (Figure 8, left part).

In the same excitation conditions (381 nm) and at the same temperature (−10 °C), the profiles of the apparent rotational correlation times ϕ as a function of the substitution position parallel those obtained in the absence of cholesterol (Figure 8, right part). For the 2- and 7-AS probes, the slight increase of the ϕ values is a function of the cholesterol mole fraction. For 9- and 12-AS, the ϕ values at 0.2 and 0.33 cholesterol mol fractions are identical within the experimental error. The peak observed for 12-AS in pure POPC vesicles as compared to 9-AS and 16-AP is more pronounced when cholesterol is present. Finally, no effect of cholesterol is evidenced for 16-AP. At 10 °C, the same remark as in pure POPC vesicles applies concerning the difficulty in the choice of a model function to fit the experimental anisotropy profiles. The variations of r_∞ and $r_{t=0}$ (Table I) are parallel.

Fluorescence Properties of DPH in Pure POPC and POPC–Cholesterol Vesicles. In Figure 9 is shown the thermal dependence of the steady-state anisotropy of DPH in pure POPC vesicles and POPC–cholesterol vesicles (0.2 mol fraction). The phase-transition temperature of POPC occurs at −3 to −4 °C. The phase transition of POPC as detected by DPH exhibits a lower degree of cooperativity than the transition of DPPC followed by the same probe (Kawato et al., 1978; Vincent & Gallay, 1983). A similar effect on the cooperativity upon introduction of single monounsaturated acyl chain was noticed by DSC (Chen & Sturtevant, 1981). The presence of cholesterol lowers the r values in the gel phase while an enhancement is observed in the liquid-crystalline phase.

In pure POPC vesicles, the total intensity decay curves of DPH are biexponential (Table III), and a significant decrease of the mean excited state lifetime $\langle\tau\rangle$ occurs when the temperature is changed from −10 to 10 °C. The presence of cholesterol does not change the value $\langle\tau\rangle$ below the transition while it increases it above (Table III).

The fluorescence anisotropy decays of DPH in POPC vesicles (at 10 or −10 °C, with or without cholesterol) are fitted with one exponential function plus a constant. The order parameter of the probe, S (Heyn, 1979; Jähnig, 1979), and the semiangle of the wobbling cone, θ_{max} (Kinosita et al., 1977), were computed. The S values reflecting the degree of packing of the fatty acid chains are especially high in the gel phase (−10 °C) (Table III). Cholesterol has no effect on S and θ_{max} values in the gel phase. In the liquid-crystalline phase (10 °C), cholesterol evokes an increase in S and a decrease in θ_{max} (Table III).

Concerning the θ_{max} values, they are relatively high for this probe, probably due to the low temperature range used in this study. The presence of cholesterol leads to a slight decrease of this parameter at −10 °C and a more important one at 10 °C (Table III).

As the last point, it is worth underlining the high value of $r_{t=0}$ especially at −10 °C (Table III). The value obtained for steady-state anisotropy of DPH in the absence of motion (i.e., $r_0 = 0.384$ in propylene glycol at −52 °C; Gallay et al., 1982) is nearly reached at this temperature (Table III).

Discussion

The physical state of membrane lipids can be characterized by different techniques. The physical parameters describing the nature of the molecular interactions between the membrane components have been unified in a single common concept: the so-called "membrane fluidity". More precisely, this concept includes (i) the orientational order of the acyl chain taken as a whole or as each of its segments, (ii) the rotational diffusion rate of the same entities, and (iii) the translational diffusion rate. Provided that time-resolved measurements are performed, the fluorescence anisotropy technique can give informations about the average orientational order and the rate of rotational diffusion in the nanosecond time scale. This study evidences that the *n*-(9-anthroyloxy) fatty acid derivatives can report on these two important physical parameters at different levels through the membrane as a function of unsaturation and cholesterol content, especially in the gel phase.

As compared to their behavior in DPPC vesicles, this set of probes exhibits important distinguished features in POPC vesicles. These differences cannot be ascribed to the presence of glycerol used as cryoprotectant, since the transition temperature evaluated with DPH as probe lies in the range of −3 to −4 °C as previously observed by DSC in the absence of cryoprotecting agent (de Kruijff et al., 1973). In the present study, control experiments performed above 0 °C with DPH gave values of r_∞ and ϕ not significantly different with or without glycerol (data not shown). Furthermore, it has been recently shown that glycerol can substitute for water in lecithin bilayer. Many physical parameters of the bilayer remained unchanged even in pure glycerol as far as the lipids are in the liquid-crystalline phase (McDaniel et al., 1983). These parameters included the thickness of the bilayer, the apparent

molar heat capacity, the temperature, and the enthalpy change of the gel → liquid crystalline phase transition.

POPC and POPC–Cholesterol. (A) Gel Phase. In this phase, like in DPPC, the out-of-plane mode of rotation of the fluorophore (monitored at 319-nm excitation wavelength where $r_0 = 0.1$) (Vincent et al., 1982a) is unhindered. It was assumed that this mode of rotation was most likely occurring primarily around the ester linkage (Vincent et al., 1982a). In POPC, in contrast to DPPC, the profile of the variation of ρ_{op} as a function of the substitution position exhibits a maximum in the region of the seventh carbon. The addition of cholesterol enhances the frictional forces in this region of the bilayer and also in ninth carbon region as was observed in DPPC (Vincent et al., 1982b), but the present study does not exclude the assumption of a close 9-(anthroyloxy) fatty acid–cholesterol association due to packing restrictions of the two ring systems in the lipid matrix as suggested by Thulborn & Beddard (1982).

The in-plane mode of rotation of the fluorophore is hindered as shown by the existence of a nonzero value in the anisotropy profile at time long after the pulse (excitation wavelength 381 nm). It was suggested that this value (r_∞) reflects the packing or the average ordering of the fatty acyl chain (Vincent et al., 1982a). In POPC gel phase, in contrast to DPPC where r_∞ is constant through bilayer, the probes detect three different zones of ordering across the membrane. From the polar interface to the double-bond region an increase in the packing is observed. In the cis double bond region a decrease of packing occurs. In the center of the bilayer the packing is higher again. As far as the double bond region is concerned, these results are similar to those of Seelig & Seelig (1977) obtained in the liquid-crystalline phase by deuterium NMR: a decrease in order parameter for 10th and 11th carbon was noticed. In the three regions, the variation of the apparent correlation time (ϕ) occurs in the opposite way as the ordering. The significance of ϕ was previously discussed (Vincent et al., 1982a). It would reflect both the in-plane and out-of-plane modes of rotation. Due to experimental limitations, the separate computation of the respective time component for each mode of rotation is not possible. However, the plots of ϕ and ρ_{op} as a function of the substitution position are not similar. Therefore, the variation of ϕ is likely to reflect the modification of the in-plane mode of rotation. Consequently, whenever the in-plane mode of rotation is more hindered, its rate of rotation is faster. The presence of a cis double bond could create a packing defect in the all-trans configuration of the CH_2–CH_2 bonds resulting from the kinked structure of the unsaturated acyl chain. This is observable not only on the dynamic properties of each phase but also on the thermodynamic characteristics of the phase transition: the unsaturated system exhibits a considerable lower transition temperature, a smaller cooperativity, and a lower transition enthalpy (Davis & Keough, 1983). A larger molecular area was also observed in monomolecular films of unsaturated lipids as compared to saturated species (Demel et al., 1972; Ghosh & Tinocco, 1972). The introduction of a large volume defect would allow a higher degree of freedom in the region between the double bond and the methyl end. A decrease of order is therefore expected in this region. On the other hand, due to its chemical structure, the double bond cannot execute rotational jumps as carbon–carbon single bonds do (Seelig & Waespe-Sarcevic, 1978). This effect is propagated in a different way toward the three regions of the chain. In this line, low hindrances exerted on the probe motion are not uncompatible with high collision frequencies. Pulse fluorometry allows a separation of these two components, which are included in the bulk "fluidity" concept.

The presence of cholesterol in POPC vesicles alters the characteristic profile of r_∞ as a function of the substitution position, due to the presence of the 9–10 cis double bond. The resulting profile is similar to the one observed in DPPC–cholesterol systems (Vincent et al., 1982b). A strong disordering effect of cholesterol is observed with 16-AP. This spacing effect was also observed in DPPC (Vincent et al., 1982b). The profile of the apparent correlation time ϕ is not strongly affected by cholesterol although all the values are slighly higher.

It is worth remarking that DPH is much less sensitive to the spacing effect of cholesterol than 16-AP. This is likely to be explainable by the different chemical structure of the probes. DPH is a rather stiff rod-shaped molecule with its long axis aligned along the acyl chain at least when the phospholipids are in the gel state (Prendergast et al., 1981). Therefore, it reports an ordering averaged over a large segment of the acyl chain. 16-AP is in contrast a flexible fatty acid. The fluorescent moiety is located only at the end of the acyl chain. Therefore, the more specific CH_3 region of the bilayer is reported by this last probe in a rather independent way from the other segments of the acyl chain. On the other hand, in isotropic solvents it was shown that the degrees of rotational freedom of the fluorescent moiety in 16-AP were higher than the other anthroloxy probes (Vincent et al., 1982a). Therefore, this probe can be also essentially more sensitive than DPH to the spacing effect of cholesterol.

(B) Liquid-Crystalline Phase. When both the in-plane and out-of-plane rotations contribute to the depolarization (381-nm excitation wavelength), the high values of the MWR, whatever the model used, preclude a quantitative interpretation of the results. These high values most probably arise either from the multiexponential form of the total intensity decay or from the complexity of the depolarizing motions:

(i) Heterogeneity analysis of the total intensity decay and its incidence on the physical meaning of the anisotropy parameters in terms of dual location have been discussed previously (Kinosita et al., 1981; Gallay et al., 1982). However, concerning the *n*-(9-anthroyloxy) fatty acids, it is not possible to distinguish between a multiplicity of sites and a solvent relaxation process (Matayoshi & Kleinfeld, 1981). Time-resolved fluorescence spectra could be used to determine the time course for the interaction since multiple sites with static interactions will not change the fluorescence with time (Thulborn & Beddard, 1982).

(ii) In any case, it is observed that the computed $r_{t=0}$ values (considered in the deconvolution process as a free parameter) are significantly lower than the steady-state r_0 values obtained in propylene glycol at −50 °C (Vincent et al., 1982a). This feature is compatible with the loss of a fast component (<1 ns) in the anisotropy decay that is not measurable with short-pulse excitation sources [either synchrotron radiation (Vincent et al., 1982a) or laser source (Thulborn & Beddard, 1982)]. In the gel phase we can assumed that the contribution of this short component in the anisotropy decay is negligible as compared to the value of the long or infinite component. It seems not to be the case in the liquid-crystalline phase where the weighing of each component is such that the contribution of the short one becomes quite important but not enough to be accurately determined. The reiterative nonlinear least-squares regression process has not sufficient information in the short time window of the anisotropy decay with regard to the tail, and a "compromise" is obtained by starting the best

fitted anisotropy curve from a $r_{t=0}$ value lower than the true one. This assumption seems to us compatible with the relatively high values of the χ^2 in the liquid-crystalline phase.

As for planar aromatic fluorophores, the fluorescence depolarization is assumed to be the result of three principal modes of rotation: two out-of-plane and one in-plane mode of rotation (Weber, 1971). The above-mentioned fast component could be assigned to one of the out-of-plane mode of rotation. This rotation would be observed mainly in the fluid phase where the differences between the r_0 values in propylene glycol at −50 °C and the computed $r_{t=0}$ are the highest. Therefore, more complex models have to be tried for the anisotropy curves: sum of three exponentials or nonexponential decays (Monnerie, 1982). Thus, in the following, the discussion will be restricted to the out-of-plane mode of rotation monitored in the fluorescence steady-state configuration with 319-nm excitation wavelength.

This mode of rotation remains unhindered either in the absence or in the presence of cholesterol. In absence of cholesterol, the absolute values of the out-of-plane correlation time, ρ_{op}, are higher in POPC than in DPPC for each probe. This difference can be the result of the higher temperature needed to induce the gel → liquid crystalline phase transition of the saturated system. Such a difference between the two crystalline phases is also evidenced with DPH. In the steady-state mode, the anisotropy values of DPH in DPPC liquid-crystalline phase was 0.082 (Vincent & Gallay, 1983) whereas in POPC liquid-crystalline phase the r value is 0.172. This difference in r value is attributable to the higher value of the wobbling-in-cone diffusion of the probe in POPC since the respective values of order parameters are similar in both systems. These differential features of the liquid-crystalline states are likely to reflect the existence of stronger frictional forces exerted on the rotational motion of the probe in POPC as compared to DPPC. In POPC–cholesterol system, ρ_{op} of 7-, 9-, and 12-AS exhibits higher values than in pure POPC. A maximum effect is observed at C_7 to C_9. The effect of cholesterol seems to be stronger in POPC than in DPPC (Vincent et al., 1982b).

Conclusions

The introduction of a single cis double bond in a lipid bilayer induces specific modifications on the dynamics and order along the acyl chain. The *n*-(9-anthroyloxy) fatty acids are sensitive to these effects. Specific results were obtained in the gel phase where these probes allow the description of three global regions: the upper part of the bilayer, the double bond region, and the acyl chain tail. The probe ordering and motion vary in an opposite way in these three regions. Addition of cholesterol at a temperature where the pure lipid is in the gel state evokes a decrease in ordering in the C_{16} region, whereas the apparent correlation time is not strongly changed. In the double-bond region, C_7 to C_{12}, the ordering becomes higher but varies as a function of the substitution position in a comparable manner as in the pure lipid. In this region the apparent correlation time values are only slightly increased upon cholesterol addition. In the polar region, the gradient of ordering from C_2 to C_7 is steeper after cholesterol addition, and the apparent correlation time values are higher.

Acknowledgments

We are indebted to D. Paillares for careful correction of the English and to B. de Foresta for reading and criticizing the manuscript. We also thank T. Montenay-Garestier (INSERM U201) for making available to us her single photon counting fluorometer during the revision of the manuscript, in order to answer to one of the referees, our own apparatus being out of order during this period.

Registry No. POPC, 26853-31-6; cholesterol, 57-88-5.

References

Chen, S. C., & Sturtevant, J. M. (1981) *Biochemistry 20*, 713–718.

Chen, L. A., Dale, R. E., Roth, S., & Brand, L. (1977) *J. Biol. Chem. 252*, 2163–2169.

Dale, R. E., Chen, L. A., & Brand, L. (1977) *J. Biol. Chem. 252*, 7500–7540.

Davis, P. J., & Keough, K. M. W. (1983) *Biochemistry 22*, 6334–6340.

De Kruijff, B., Demel, R. A., Slotboom, A. J., Van Deenen, L. L. M., & Rosenthal, A. F. (1973) *Biochim. Biophys. Acta 307*, 1–19.

Demel, R. A., Guerts van Kessel, W. S. M., & Van Deenen, L. L. M. (1972) *Biochim. Biophys. Acta 266*, 26–40.

Evans, R. W., & Tinocco, J. (1978) *Chem. Phys. Lipids 22*, 207–220.

Gallay, J., Vincent, M., de Paillerets, C., Rogard, M., & Alfsen A. (1981) *J. Biol. Chem. 256*, 1235–1241.

Gallay, J., Vincent, M., & Alfsen, A. (1982) *J. Biol. Chem. 257*, 4038–4041.

Ghosh, D., & Tinocco, J. (1972) *Biochim. Biophys. Acta 266*, 41–49.

Griffith, O. H., & Jost, P. C. (1976) *Spin Labeling, Theory and Applications* (Berliner, L. J., Ed.) pp 454–523, Academic Press, New York.

Haigh, E. A., Thulborn, K. R., & Sawyer, W. H. (1979) *Biochemistry 18*, 3525–3532.

Heyn, M. P. (1979) *FEBS Lett. 108*, 359–364.

Jähnig, F. (1979) *Proc. Natl. Acad. Sci. U.S.A. 76*, 6361–6365.

Kawato, S., Kinosita, K., & Ikegami, A. (1978) *Biochemistry 17*, 5026–5031.

Kinosita, K., Kawato, S., & Ikegami, A. (1977) *Biophys. J. 20*, 289–305.

Kinosita, K., Jr., Kawato, S., Ikegami, A., Yoshida, S., & Orii, Y. (1981) *Biochim. Biophys. Acta 647*, 7–17.

Kremer, J. M. H., Esker, M. W., Pathmamanoharan, C., & Wiersema, P. H. (1977) *Biochemistry 16*, 3932–3935.

Lakowicz, J. R., & Knutson, J. R. (1980) *Biochemistry 19*, 905–911.

Lentz, B. R., Barenholz, Y., & Thompson, T. E. (1976) *Biochemistry 15*, 4521–4528.

Lipari, G., & Szabo, A. (1980) *Biophys. J. 30*, 489–506.

Matayoshi, E. D., & Kleinfeld, A. M. (1981) *Biophys. J. 35*, 215–235.

McDaniel, R. V., McIntosh, T. J., & Simon, M. A. (1983) *Biochim. Biophys. Acta 731*, 97–108.

Monnerie, L. (1982) in *Photophysics of Synthetic Polymers* (Phillips, D., & Roberts, A. D., Eds.) Science Review Ltd., Northwood, England.

Prendergast, F. G., Haugland, R. P., & Callahan, P. J. (1981) *Biochemistry 20*, 7339–7345.

Seelig, J. (1977) *Q. Rev. Biophys. 10*, 353–418.

Seelig, A., & Seelig, J. (1977) *Biochemistry 16*, 45–50.

Seelig, J., & Waespe-Sarcevic, N. (1978) *Biochemistry 17*, 3310–3315.

Stubbs, C. D., Kouyama, T., Kinosita, K., & Ikegami, A. (1981) *Biochemistry 20*, 4257–4262.

Thulborn, K. R., & Sawyer, W. H. (1978) *Biochim. Biophys. Acta 511*, 125–140.

Thulborn, K. R., & Beddard, G. (1982) *Biochim. Biophys. Acta 693*, 246–252.

Valeur, B. (1978) *Chem. Phys. 30*, 1–11.
Vincent, M., & Gallay, J. (1983) *Biochem. Biophys. Res. Commun. 113*, 799–810.
Vincent, M., de Foresta, B., Gallay, J., & Alfsen, A. (1982a) *Biochemistry 21*, 708–716.
Vincent, M., de Foresta, B., Gallay, J., & Alfsen, A. (1982b) *Biochem. Biophys. Res. Commun. 107*, 914–921.
Weber, G. (1971) *J. Chem. Phys. 55*, 2399–2407.
Zannoni, C., Arcioni, A., & Cavatorta, P. (1983) *Chem. Phys. Lipids 32*, 179–250.

Cooperative Interactions in the System Ribosomes–Ribosomal Protein S1–Polynucleotide Triplets†

Dixie J. Goss, Lawrence J. Parkhurst,* Arkesh M. Mehta, and Albert J. Wahba

ABSTRACT: Association equilibria have been determined in the ternary system uridyl triplets (T)–ribosomal protein S1 (S)–ribosomes (Rb) depleted of S1 at 6 and 10 mM Mg^{2+}. For 1:1 stoichiometry of reactants, four thermodynamically independent equilibria characterize the ternary system. The binary interaction Rb + T was studied by following the fluorescence quenching of labeled ribosomes by added T. The Rb + T association constant for UpUpUp triplets was 10–20-fold greater than for ApUpG triplets. The interaction Rb + S was studied by following the changes in fluorescence anisotropy when labeled S1 reacted with ribosomes. The remaining two independent equilibrium constants (for S + T and RbT + S) were obtained from fits to observed anisotropy measurements when varying amounts of T were added to a solution of ribosomes and fluorescently labeled S1. This indirect procedure allows one to measure S + T binding, an association that is difficult to determine directly. Over the concentration interval 5–10 mM Mg^{2+}, the association constant for Rb + S increases with the sixth power of $[Mg^{2+}]$, whereas the association constant for S + T *decreases* approximately 2-fold as Mg^{2+} is increased from 6 to 10 mM Mg^{2+}. T binds to Rb more tightly at 10 mM than at 6 mM Mg^{2+}. When S1 is bound to Rb, however, at 10 mM Mg^{2+} the binding constant for T is *decreased* 10-fold and the Mg^{2+} dependence is reversed. These interactions can be described in terms of coupling free energies. For the ternary complex, three linearly independent coupling free energies can be written. These excess functions simply show by how much we err in estimating the overall free-energy change for formation of the RbST complex from free-energy changes for the formation of various binary fragments. One of the ternary coupling free energies, $\Delta G^\circ_{R,ST}$ ($=\Delta G^\circ_{RST} - \Delta G^\circ_{RT} - \Delta G^\circ_{RS}$), is positive (anticooperative interaction) at 10 mM Mg^{2+} but negative at 6 mM Mg^{2+}, primarily because of the sensitivity of ΔG°_{RS} to $[Mg^{2+}]$. Thus, at 6 mM Mg^{2+}, prior binding of S1 to the ribosome enhances binding of the triplet to form the ternary complex, but at 10 mM Mg^{2+}, S1 binding to Rb destabilizes subsequent binding of the triplet. More elaborate models that assumed multiple sites for T on S and Rb were used to fit the data; however, both the anisotropy data and the results for triplet quenching of ribosome fluorescence were in accord with a simple description where the binding of the triplets to the ribosome appeared to be to a single site. If there are multiple sites for triplet binding, the binding sites show little interaction or heterogeneity over the concentration ranges studied. Our results lend support to assigning primary importance to protein–protein interactions in the binding of S1 to the ribosome. Although S1 may well function as an unwinding protein, it can profoundly affect the binding of nonhelical trinucleotides to the ribosome.

Although there have been many studies of protein synthesis initiation, there is still not a clear understanding of this process on a molecular level. What are the control mechanisms for this process? Koshland et al. (1983) have pointed out that biological organisms must respond to their environment on a cellular level. Cells must "turn on" or "turn off" various processes in response to external signals. These biological systems require the amplification of some stimuli and the ability to adapt to background levels of other stimuli. The amplification and adaptation can be achieved in a variety of ways, among them are cooperative interactions of molecules, multistep input of regulators, allosteric effectors, and covalent modification of the proteins.

In order to determine possible control points for protein synthesis initiation, we have examined some of the simpler molecular interactions and the role of possible effectors. The simplest interactions are the binary interactions such as 70S ribosome dissociation and subunit association, the binding of IF3 to ribosomes, mRNA binding to ribosomes, and S1 binding to ribosomes. The interactions become more complex for ternary and higher order interactions. We describe here the equilibrium interactions for ribosomes (Rb), ribosomal protein S1 (S), and nucleotide triplets (T) at 6 and 10 mM Mg^{2+}. We have considered a number of different models for these interactions. The simplest model assumes (1) S1 has one nucleotide triplet binding site, (2) ribosomes have one S1 binding site, and (3) there is effectively one nucleotide triplet binding site on the ribosome. Because of a variety of sometimes conflicting evidence in the literature, we have examined more complex models as well.

Our data could be fit well with the simple model. However, just as simple models for IF3 interaction, such as the antiassociation model, were sufficient for early data (Dondon et al., 1974; Godefroy-Colburn et al., 1975; Gottlieb et al.,

† From the Department of Chemistry, University of Nebraska, Lincoln, Nebraska 68588-0304 (D.J.G. and L.J.P.), and the Department of Biochemistry, University of Mississippi Medical Center, Jackson, Mississippi 39216 (A.M.M. and A.J.W.). *Received October 13, 1983.* We thank the following agencies for support of this research: National Institutes of Health (Grants HL 15,284 and GM 25451), National Science Foundation (Grant PCM 8003655), and Research Council, University of Nebraska.

0006-2960/84/0423-6522$01.50/0